Title
The spatial arrangement of L and M cones in the peripheral human retina

Journal
Vision Research, 40(6)

ISSN
0042-6989

Authors
Otake, Shiro
Gowdy, Peter D
Cicerone, Carol M

Publication Date
2000-03-01

DOI
10.1016/s0042-6989(99)00202-3

PERGAMON

Vision Research 40 (2000) 677–693

Vision Research

www.elsevier.com/locate/visres

The spatial arrangement of L and M cones in the peripheral human retina

Shiro Otake [1], Peter D. Gowdy [2], Carol M. Cicerone *

Department of Cognitive Sciences, University of California, Irvine, CA 92697-5100, USA

Received 14 October 1997; received in revised form 14 August 1998

Abstract

The spatial arrangement of L and M cones in the human peripheral retina was estimated from red–green color naming of small test flashes (0.86 min of arc, 555 nm, constant intensity) presented at different locations (grid with 1.5 min of arc steps) centered at 17° temporal eccentricity. Simulated red–green color naming ratings were generated by a model based on an ideal observer for all possible patterns of placement and relative numerosities of L and M cones, constrained by the anatomical data on the statistics of cone spacing at this retinal location. The best matching simulated performance as compared to the human observer's data determined the cone array most likely to produce that observer's color naming results. The mosaics for two color normal observers showed L and M cones randomly arrayed over this retinal region. Consequences of random cone placements for spectral sampling and color opponency are discussed.

Keywords: Cone; Peripheral retina; Topography

1. Introduction

1.1. Background

Human color vision originates in signals from three classes of cone photoreceptors whose spectral sensitivities are well-established (Marks, Dobelle & MacNichol, 1964; Smith & Pokorny, 1975; Schnapf, Kraft & Baylor, 1987; Stockman, MacLeod & Johnson, 1993). Changes in the density of the total number of cones with retinal eccentricity (Østerberg, 1935; Williams, 1988; Curcio, Sloan, Kalina & Hendrickson, 1990) and the distribution of the subpopulation of short-wavelength-sensitive (S) cones (Ahnelt, Kolb & Pflug, 1987; Curcio, Allen, Sloan, Lerea, Hurley, Klock & Milam, 1991) are also well known. Furthermore, the anatomical estimates of the S cone distribution show close correspondence to psychophysical estimates in humans (e.g. Williams, MacLeod & Hayhoe, 1981; Castaño & Sperling, 1982) as well as to the distribution of S cones found in other primates (Marc & Sperling, 1977; de Monasterio, Schein & McCrane, 1981; Mollon & Bowmaker, 1992). By comparison to the well-established distribution of S cones, distribution and spatial arrangements of the L and M cones in the human retina are not as well established. Anatomical assays of the distributions of long- (L) and middle-wavelength-sensitive (M) cones have been obtained in nonhuman primate retina (Marc & Sperling, 1977; Mollon & Bowmaker, 1992; Packer, Williams & Bensinger, 1996) but not for the human retina, in part because these two types share morphological (Ahnelt et al., 1987; Curcio et al., 1991) and genetic (Nathans, Thomas & Hogness, 1986) characteristics. Recently devised techniques estimate more L cones than M cones in the color normal human retina (Cicerone & Nerger, 1989; Vimal, Pokorny, Smith & Shevell, 1989; Nerger & Cicerone, 1992; Hagstrom, Neitz & Neitz, 1998; Gowdy & Cicerone, 1998; Roorda & Williams, 1999). Whether these two classes of cones pave the photoreceptor mosaic in regular, clumped, or random arrays is a current focus of interest, because this information is required to under-

* Corresponding author. Fax: +1-949-824-2307.

E-mail address: cciceron@uci.edu (C.M. Cicerone)

[1] Present address: Corporate Research Division, Matsushita Electric Industrial Co., Ltd., 3-4 Hikari-dai, Seika, Soraku7, Kyoto 619-02, Japan.

[2] Present address: Division of Engineering and Applied Sciences and Department of Psychology, Harvard University, Cambridge, MA 02138, USA.

0042-6989/00/$ - see front matter

PII: S0042-6989(99)00202-3

stand how the cone quantum catches are transformed into the neural signals subserving color appearance. Using a procedure combining psychophysical measurements and a model based on an ideal observer, this study concludes that the L and M cones are randomly distributed in the photoreceptor matrix of the peripheral retina of the living human eye.

1.2. General approach

The psychophysical method used in this study is based on long-standing reports that foveal presentations of a small (ca. 1 min of arc), dim spot of light of unvarying wavelength and luminosity can vary dramatically in color appearance from flash to flash (Holmgren, 1884, 1889; Fick, 1888; Hartridge, 1947; Walraven, 1962; Krauskopf, 1964; Cicerone & Nerger, 1989). For foveal flashes, trial-to-trial changes in color appearance are likely due to illumination of different clusters of five to seven cones (e.g. Marriott, 1963; Geisler, 1984; Cicerone & Nerger, 1989), not single cones on any flash, because of the limitations imposed by diffraction and by the optical spread of light over the tightly packed foveal cone array. It was reasoned here that presentation of such small, dim lights in the peripheral retina should enhance the likelihood of illumination of single cones, certainly fewer cones than in the fovea, because the cones are spaced at a larger distance from their neighbors. In principle then, changes in color appearance for different flash locations in the peripheral retina could be used to estimate the spatial arrangement of different cone types in the overall photoreceptor matrix by linking the pattern of responses to the cone mosaic most likely to account for the data.

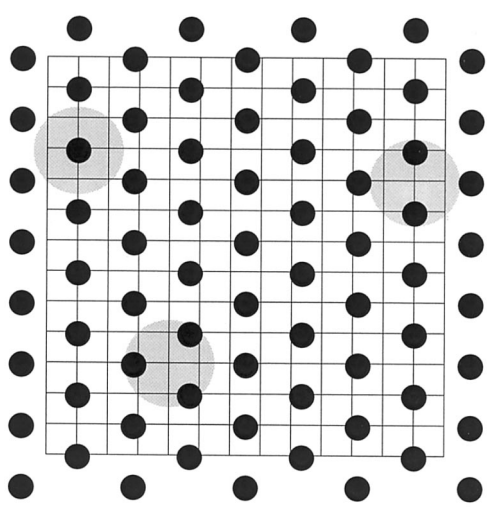

Fig. 1. A hypothetical array of cones at 17° temporal eccentricity in the human retina is shown in relationship to the locations of the test light. The cones (closed circles) are separated by 3 min of arc, on average, in an array whose arrangement roughly approximates the perfect hexagonal array shown here. The test (0.86 min of arc, 50 ms, 555 nm, self-presented, adjusted to an intensity seen 80–90% of the time to minimize scattered light) remained the same from trial to trial; only its location was varied, over a region spanning 19.5 min of arc square, in steps of 1.5 min of arc (shown as one unit of the grid). At each test location, represented by each intersection of the grid lines, the observer judged the color appearance of the test. The shaded regions show the effective area of illumination for three prototypical locations of the test. Assuming a perfect triangular lattice, if the test is centered upon a cone, only that cone is involved in detection or determination of color appearance. If the test falls among the cones, no more than three cones are likely to contribute to the determination of color appearance. (See text for more details.)

The choice of region in peripheral retina was guided by the following: First, anatomical estimates of cone density show a sharp decline in the density of cones from fovea centralis to 17° eccentricity, where the center-to-center spacing of the cones is approximately 3 min of arc and thereafter remains roughly constant (Curcio et al., 1990). Second, studies on trial-to-trial fixational accuracy (Williams et al., 1981; McKee & Levi, 1987; Fahle, 1991; Gowdy & Cicerone, 1998) indicate that the 3 min of arc spacing of cones in this retinal region significantly exceeds the standard deviation of fixational accuracy, estimated to range between 0.5 and 2.5 min of arc. Third, a recent study (Navarro, Artal & Williams, 1993) on the image quality of the eye measured with natural pupil and natural accommodation indicates that 'the optical quality in the fovea is not particularly good when compared with conventional optical systems, but it shows relatively good off-axis behavior, maintaining relatively constant quality with eccentricity over a wide visual field. Only the far periphery shows a large decline in image quality'. The foveal results are in good agreement with Campbell and Gubisch's results for a 3.8 mm pupil. The aerial point spread functions measured in four individuals in the study by Navarro et al. (1993, Fig. 2) are virtually unchanged up to 10° eccentricity with a modest decline in quality at an eccentricity of 20° and significant loss of optical quality for eccentricities greater than 30°. All of these factors motivated the choice of this peripheral region as most suited for our observations with small, dim test flashes of light designed to obtain color naming based on a small number of cones.

The general strategy is sketched in Fig. 1. The test flash locations (grid intersections) are separated by steps of 1.5 min of arc or half of the mean center-to-center separation among cones in this region of the retina. Each cone requires at least 5–10 quanta to be activated according to a number of psychophysically and electrophysiologically based estimates (Marriott, 1963; Cicerone & Nerger, 1989; Schnapf, Nunn, Meister & Baylor, 1990). If a near threshold, small (< 1 min of arc) test light is centered upon a cone, each of its nearest neighbors is illuminated by insufficient numbers of quanta to contribute to detection or to determination of color appearance, according to the optical scat-

ter profile (Campbell & Gubisch, 1966) assumed for this purpose. (This assumption is discussed more fully in Section 2.2.) If the test falls among the cones, no more than three cones are likely to contribute to the determination of color appearance. For illustrative purposes, cone photoreceptors are shown to lie in a perfectly hexagonal array with 3 min of arc cone-to-cone spacing. In the analysis detailed below, departures from a perfectly hexagonal array are considered.

In the present experiments, a test wavelength of 555 nm was chosen because it is virtually equal in its effectiveness for individual L and M cones. When a small (0.86 min of arc) test flash of wavelength 555 nm and constant, near threshold intensity was moved from location to location in this region of peripheral retina centered at 17° temporal eccentricity, observers reported changes in color appearance ranging from red to yellow to green, of varying saturation. As the test location is changed, presumably illuminating different groups of the three cone classes, flashes are likely to appear red if quantal absorptions are predominantly in L cones, green from absorptions in M cones, and yellow from significant absorptions in both types (Jameson & Hurvich, 1955; DeValois, 1965; Wiesel & Hubel, 1966; Larimer, Krantz & Cicerone, 1974). Experiments confirmed that the spectral sensitivity measured in locations named green best matched the spectral sensitivity of M cones and in locations named red best matched that of L cones. It was reasoned, therefore, that location-specific color naming of a small spot test — moved across the area at 17° temporal eccentricity in steps of half the mean center-to-center spacing of cones — could be linked to the spatial positions of the individual cones in the photoreceptor array with a suitable model of color naming. The ideal-observer based model (Green & Swets, 1966), located at the color opponent site, generated color ratings by considering all possible spatial arrangements and all possible relative numerosities of the L and M cones. The cone arrays were constrained by the available anatomical estimates of the statistics of cone spacing at this retinal region (Curcio et al., 1991). Each observer's mosaic was determined by the simulated performance, generated by the model, that most closely matched the human observer's performance. For one observer, this analysis was applied to different color naming observations obtained in separate sessions for the same region of retina. The derived test and retest mosaics are similar, thus adding to confidence in the method. Finally, statistical analyses (Ripley, 1981) were applied to each observer's mosaic to determine whether the separate L and M cone arrays conformed to random, clumped, or regular distributions.

2. Experiment 1. Threshold measurements and choice of rod suppressing conditions

The choice of a peripheral retinal region centered at 17 temporal eccentricity gained the advantage of relatively large cone center-to-center separations without significant loss of optical quality as compared to the optic axis, as explained in Section 1.2. On the other hand, in this peripheral region of the retina, in addition to L and M cones, there are abundant rods and a few S cones which must be considered. In order to exclude rod participation in this rod-rich area, measurements were made after a rod bleach and upon a dim 460 nm background, designed to keep the sensitivity of the rods at a level well below that of the L and M cones (Nerger & Cicerone, 1992). Experiment 1 was designed to show that under the conditions of the experiment, there was adequate reduction of the sensitivity of rods to exclude their participation in Experiments 2 and 3. In order to ensure that the sensitivity of rods was effectively reduced by this regimen, dark adaptation was measured with a 520 nm test light, which was more likely to be detected by the rods as compared to the 555 nm light used in the color naming experiment (Experiment 2). Dark adaptation functions measured both with and without the dim 460 nm background give assurance that the sensitivity of rods was sufficiently reduced for a 20 min-period after the recovery of cones if both the rod bleach and the dim 460 nm background were used.

Although S cones comprise approximately 8% of the cone population at this eccentricity (Ahnelt et al., 1987; Curcio et al., 1991), S cones are more than three orders of magnitude less sensitive to 555 nm light as compared to L or M cones, giving assurance that S cones are unlikely to participate in the color naming task.

The 460 nm background was of low effectiveness for L and M cones and unlikely to alter cone-based color appearance. As a check, measurements of unique yellow were compared to foveal measurements in the same observer and shown to be near equal. Thus, the red–green color opponent site was unlikely to be significantly affected by either the rod bleach or the dim, 460 nm background.

2.1. Methods

2.1.1. Observers

Two color normal (as confirmed by Neitz OT anomaloscope matches) observers participated. Observer CC (female, emmetrope) was one of the authors. Observer KL (male, corrected for myopia of -2.25 D) was unaware of the purposes of the experiment.

2.1.2. Apparatus and procedures

The three-channel Maxwellian-view apparatus is shown in Fig. 2. The observer's head position was fixed

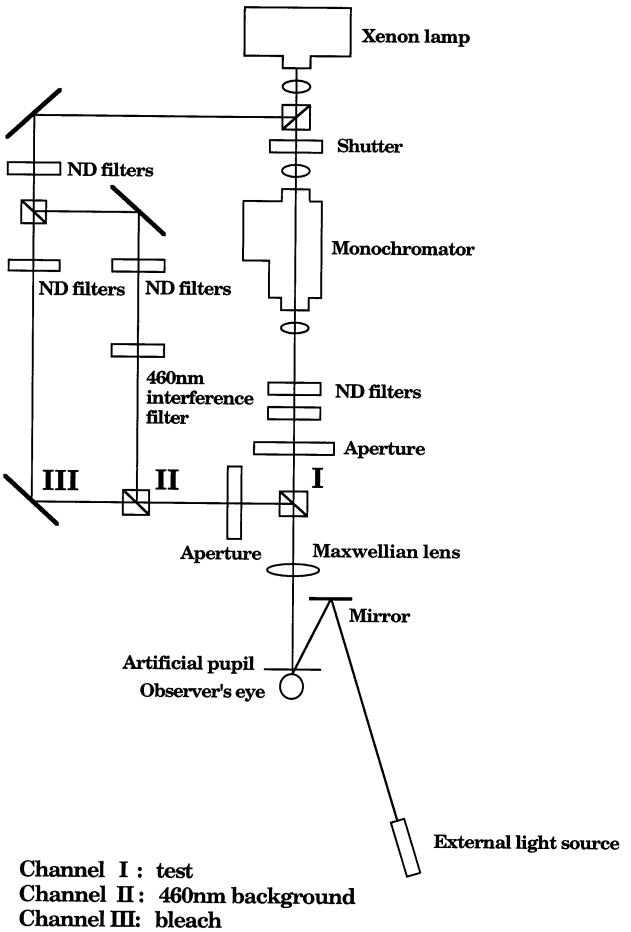

Fig. 2. The three-channel Maxwellian-view apparatus is shown. Channel I provided the test (0.86 min of arc, 50 ms duration) presented upon a rod and S cone suppressing background (460 nm, 7°, 11.3 scotopic trolands, 0.48 photopic troland) provided by Channel II. Channel III provided the rod bleaching field (broadband, 7° in diameter, 4.5 log scotopic troland applied for 10 s) estimated to bleach 40% of the rod photopigment. Apertures, neutral density (ND) and interference filters, a monochromator, shutters, lenses, a mirror, and light sources were employed as shown. An external light source provided the fixation target mounted on a micromanipulator and allowed presentation of test stimuli in various locations in a region centered at 17° temporal eccentricity. The diagram is not to scale.

by means of a bitebar, and the stimuli were monocularly viewed with the right eye through a 2.8 mm artificial pupil. Minor adjustments in the near-to-far positioning of the test aperture were made, individually for each observer, to further improve the clarity of the test stimulus. Trial lenses were tested but not used as they did not improve the clarity of the stimulus for these two observers. One channel provided a test (0.86 min of arc, 520 nm, 50 ms duration) of variable intensity. The wavelength of the test was controlled by a monochromator (Instruments SA, H-20V). The test was presented upon a rod and S cone suppressing background (460 nm, 7°, 11.3 scotopic trolands, 0.48 photopic troland) provided by a second channel. The third channel provided the rod bleaching field (broadband, 7° in diameter, 4.5 log scotopic troland applied for 10 s) estimated to bleach 40% of the rod photopigment (Alpern, 1971). An external LED provided the fixation target for test stimuli in a region centered at 17° temporal eccentricity. All optical components were anchored to an optical table (Newport Corporation, MS series). A radiometer/photometer (EG&G, Model 450) was used for all calibrations.

The rod bleaching light was applied for 10 s, after which the 460 nm background was turned on, immediately followed by test presentations upon the background. Using neutral density filter wheels in the test channel, the experimenter recorded the intensity of each test flash and its presentation time after the bleach. On each trial (one in ten a blank trial) the observer signaled whether a flash was seen. Neither observer made any false alarms. Thresholds were set at the level seen 60% of the time.

2.2. Results

Fig. 3 shows the course of dark adaptation after the rod bleach as measured with a 520 nm test for Observer

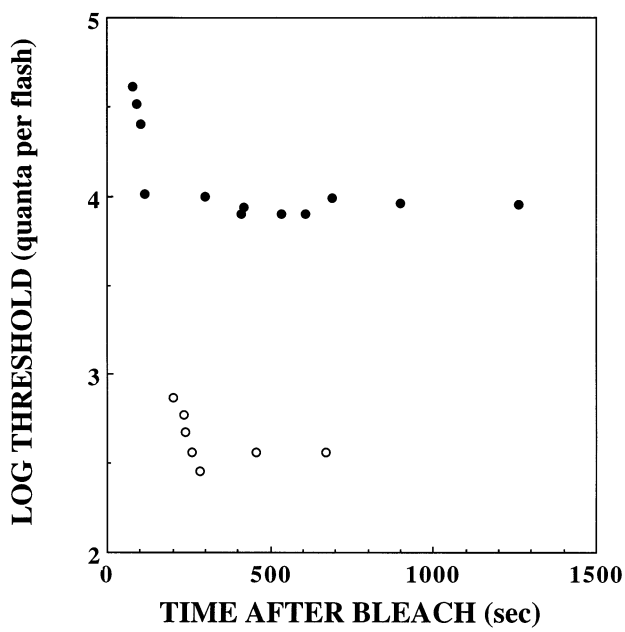

Fig. 3. The time course of dark adaptation after the 40% rod bleach for observer CC is shown. Log threshold (quanta per flash, 520 nm) is plotted as a function of time after the bleach (s). In one condition dark adaptation was measured with the rod bleach alone (open symbols) and in the second condition with the rod bleach and the steady, 460 nm background (closed symbols). Without the short-wavelength background, the rods quickly recovered their sensitivity even after the bleach, allowing little time for cone-based measurements. The bleach in combination with a steady background maintained a selective reduction of roughly 1.5 log units in the sensitivity of rods below that of the cones, while preserving the sensitivity of the L and M cones for a period of over 20 min, the length of time during which experimental measurements were made.

CC. Two conditions are plotted, one with the rod bleach alone and the other with the rod bleach and the steady, 460 nm background. The intensity of the 460 nm background, as noted in the methods above, was set to be effective for rods but barely detectable, if at all, by the cones. Without the short-wavelength background, the rods quickly recovered their sensitivity even after the 40% rod bleach, allowing little time for cone-based measurements. In line with results in the literature (Aguilar & Stiles, 1954; Arden & Weale, 1954), the bleach in combination with a steady background maintained a selective reduction, roughly 1.5 log units, in the sensitivity of rods below that of the cones, while preserving the sensitivity of the L and M cones for a period of 20 min, the duration of time over which experimental measurements were made in the subsequent experiments. The test used in subsequent experiments was of wavelength 555 nm, further ensuring that the rods did not contribute to detection.

It was estimated from the last values in the dark adaptation functions shown in Fig. 3 that for the 520 nm test, 9106 quanta were delivered by each flash at cone threshold and 363 quanta per flash for rod threshold (measured at the cornea). This is in reasonable agreement with measurements in the literature for conditions close to those in this study. For example, Marriott (1963) reported a rod threshold value of 348 quanta measured at the cornea with a 555 nm, 1.2 ms, 1 min of arc test light at 24° temporal eccentricity, similar to the conditions of the present experiment. In the present experiment the rod value is 363 quanta measured with a 520 nm, 50 ms, 0.86 min of arc test light after approximately 700 s of dark adaptation.

The luminance (11.3 scotopic and 0.46 photopic troland) of the 460 nm background was chosen to be high enough to reduce rod sensitivity but to be of low effectiveness, barely detectable, for the cones (Hecht, Haig & Chase, 1937). The combined regimen of rod bleach and low luminance chromatic background is unlikely to affect cone-based color appearance. Although changes in the red-green color opponent site due to short-wavelength chromatic adaptation have been reported (e.g. Cicerone, Krantz & Larimer, 1975), the adapting levels reported to produce changes are a 100-fold greater than that used in these experiments. Nonetheless, it could be argued that, although the 460 nm background is not likely to be detected by the L or M cones, the combined activation of all M cones as compared to all L cones illuminated by the dim 460 nm background is about 28% greater for the M cones (MacLeod & Boynton, 1979) and thus the red–green color opponent site might be affected. Measurements of unique yellow were used to check for any influence the rod-desensitizing regimen might have at the red–green color opponent site. Unique yellow measured at 17° temporal eccentricity was 576.8 nm after recovery of the cones and upon the dim, 460 nm background as compared to 577.4 nm measured in the fovea for (naive) observer KL. Thus, it is not likely that the low intensity 460 nm background affects red/green color appearance in the middle to long wavelength range of the spectrum.

3. Experiment 2. Small spot color naming in peripheral retina

The purpose of Experiment 2 was to measure changes in color appearance associated with changes in test location in a region centered at 17° temporal eccentricity and estimated to contain 72 cones (Curcio et al., 1990). As discussed above (Section 1.2) the region of retina centered at 17° temporal eccentricity was chosen for its relatively large mean spacing of the cones of 3 min of arc, center-to-center (Curcio et al., 1990). This spacing, combined with optical properties approaching that measured along the optic axis (Navarro et al., 1993) make it likely that one, two or three cones are illuminated with our small, dim test flashes (Fig. 1).

As a check of the conditions of this experiment, we first measured the number of quanta delivered at threshold (60% seen) for a 555 nm, 0.86 min of arc test light presented in the fovea. For observer CC this value was 854 quanta measured at the cornea which is in good agreement with results in the literature. For example, to estimate a foveal cone threshold ranging between 500 to 900 quanta per flash in a sample of nine observers Marriott (1963) used foveal presentations of a 550 nm light subtending 1 min of arc and of 1.2 ms duration. From his results, Marriott (1963) estimated that at least 5 quanta are required to activate a single cone.

Next, for each observer, we set the intensity of the 555 nm test to be seen 80–90% of the time when presented at 17° temporal eccentricity and after the rod bleach upon the rod-adapting 460 nm background. At this suprathreshold level the observers reported that the flashes appeared colored. By comparison, when tests are set near detection level for cones, they usually appear highly desaturated as was noted in the course of this study and by others (e.g. Marriott, 1963). As compared to the value of 854 quanta at the cornea for foveal presentations seen 60% of the time, the 555 nm test flash was estimated to deliver 3325 quanta at the cornea for peripheral presentations seen 80–90% of the time. Thus, if the flash is centered upon a cone in this peripheral region of the retina, three to four times as many quanta are estimated to be delivered as compared to the number required for detection, based on the estimates of Marriott. The relative illuminance of any cone centered at a distance of 3 min of arc (mean cone spacing for this region of the retina) from the peak of

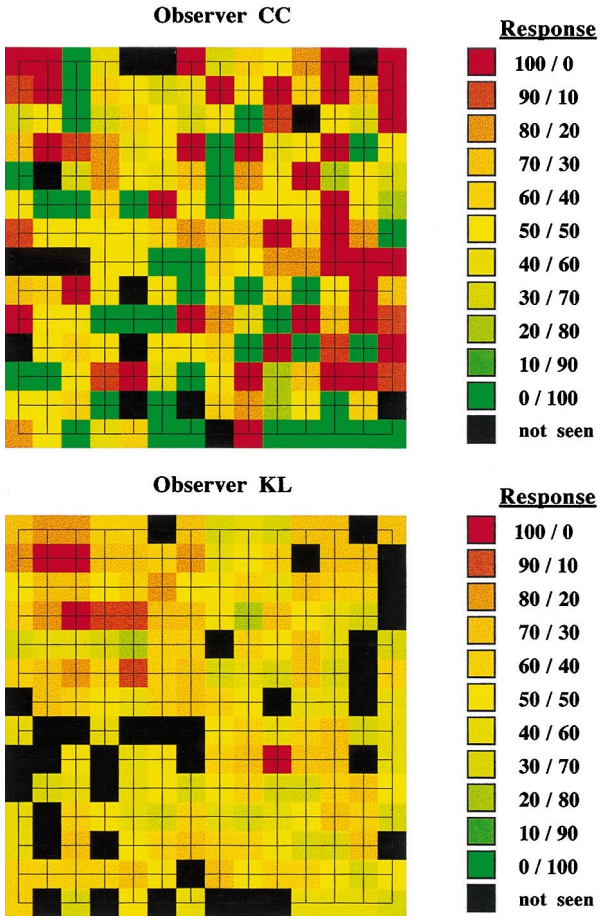

Fig. 4. Results of the small-spot color naming experiment are shown for observers CC (top) and KL (bottom). The color shown in each small square represents the judged color appearance of the test spot when presented at each test location (center of each colored square). Black squares mark locations where the test was not seen on a particular trial. More nasal retinal locations are represented toward the right in this diagram, superior locations upwards. Shown at the right are the scales for redness and greenness used by the observers.

the illumination profile is approximately 0.2 (Campbell & Gubisch, 1966). Thus, a cone centered 3 min of arc distant from the center of the test flash is likely to absorb 3–4 quanta, below the minimum value of 5 quanta estimated by psychophysical means (Marriott, 1963; Cicerone & Nerger, 1989; Vimal et al., 1989) and well below the value of 10 quanta estimated in isolated cone photoreceptors (Schnapf et al., 1990). Thus, it is plausible that few cones contribute to color naming of the small, dim test spot used in these experiments. The test flash, of unvarying wavelength and intensity, was randomly moved from location to location in a grid with spacing of 1.5 min of arc, half the mean distance between centers of cones in this retinal region. Observers rated the red–green color appearance of each flash.

3.1. Methods

3.1.1. Observers

The observers were the same as for Experiment 1.

3.1.2. Apparatus and procedures

The three-channel Maxwellian-view apparatus described above and shown in Fig. 2 was used. One channel provided a test (0.86 min of arc) of unvarying wavelength (555 nm) presented upon a rod and S cone suppressing background (460 nm, 7°, 11.3 scotopic trolands, 0.48 photopic troland) provided by a second channel. The intensity of the test was fixed at a level determined separately for each observer as that producing 80% seen for test presentations centered at 17° temporal eccentricity. The third channel provided the rod bleach. An external light source, LED mounted on a micromanipulator (Melles Griot, model 07TPD005), provided the fixation target. The high precision of the micromanipulator (0.01 mm) and the long lever arm of our external fixation source allowed 0.0264 min of arc accuracy in the placement of the fixation target.

Test location was varied by moving the fixation target. Tests were presented at each grid location in random order. On each trial the observer was instructed to press a button in order to present the test when sure of accurate fixation. The control of the experiment was aided by a computer. When the test was seen, the observer rated the redness and greenness of the small spot test according to a scale running from 0 to 100 in increments of 10, apportioning the points to sum to 100 (Boynton & Gordon, 1965; Abramov, Gordon & Chan, 1991). For example, a flash appearing entirely red was assigned 100 red and 0 green; one appearing entirely green, 0 red and 100 green; one appearing yellow, 50 red and 50 green.

3.2. Results

The results are displayed in Fig. 4 for observers CC (top) and KL (bottom). Each map is centered at an eccentricity of 17° in the temporal retina; nasal locations are plotted to the right and superior locations to the top. The color shown in each small square illustrates the judged color appearance of the test spot when presented at that test location. Black squares mark locations where the test was not seen. Observer CC used the full range of color ratings. Observer KL used the full range except for the two extreme green categories, 10/90 and 0/100. In addition, he used fewer extreme red ratings as compared to Observer CC (two as compared to 36, respectively, out of 196 test locations). These differences could be explained if observer KL has a response bias against using extreme color ratings. Alternatively, the results could be explained if

either the spacing between the cones in KL's array is smaller than CC's or the optical quality of KL's lens system is poorer, producing greater light spread than CC's. In either of these two cases, more cones are illuminated by each flash, increasing the likelihood that each flash illuminates both L and M cones.

It was reasoned that test locations yielding 100% red color ratings may be near positions of L cones and those yielding 100% green color ratings may be near positions of M cones. In the next experiment, as a test of the proposed link between small spot color naming and the composition of the underlying mosaic, spectral sensitivities are measured at these candidate L and M cone positions.

4. Experiment 3. Spectral sensitivity measurements in L-cone and M-cone-candidate locations

If red–green color naming is based on the relative absorptions in the L and M cones, then spectral sensitivities measured at locations judged wholly red (100/0) should match that of L cones and those judged wholly green (0/100) should match that of M cones. There are a number of such locations in the color naming diagram shown in Fig. 4 for Observer CC. Experiment 3, designed as a direct test of this idea, estimated spectral sensitivities at these L-cone and M-cone-candidate positions. The difficulty of repeated measurements located at a specific position in the experimental grid (Fig. 1) offered the choice of either employing many test wavelengths and few repeated presentations or a selected small number of wavelengths and many repeated presentations. The latter course was chosen — to estimate the spectral sensitivity of the cone(s) at each candidate location with two wavelengths, 520 and 620 nm — because L an M cone differences in the sensitivity to these two wavelengths are large enough to allow distinguishing these two cone types.

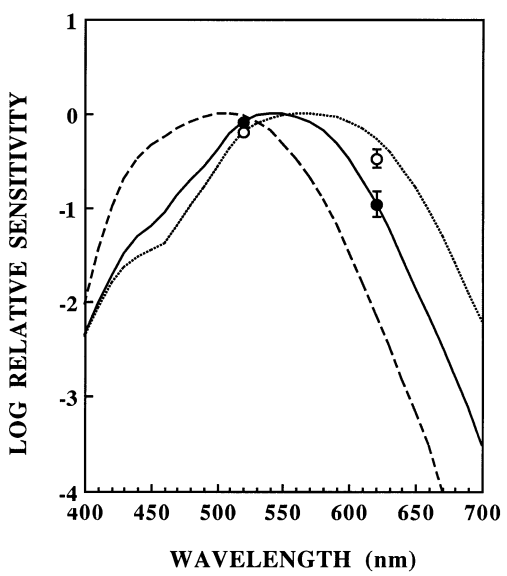

Fig. 5. Shown are the means of the relative spectral sensitivities measured at three M cone candidate locations (closed symbol) and four L cone candidate locations (open symbol) from observer CC's color naming observations (Fig. 4, top) as compared to the Smith and Pokorny (1975) L (dotted contour) and M (solid contour) cone spectral sensitivities. Also shown is the rod spectral sensitivity (dashed contour). Measurements were made at 520 and 620 nm, and the relative sensitivity to 620 nm as compared to 520 nm are plotted. The error bars mark the 95% confidence limits. Specifying the square at the lower, left corner of Fig. 4 as location (1, 1), candidate locations for M cones were at (12, 1), (4, 2), and (9, 6), and candidate locations for L cones were at (12, 13), (13, 6), (10, 8), and (2, 14).

4.1. Methods

4.1.1. Observer

The experiment was conducted with observer CC.

4.1.2. Apparatus and procedures

The apparatus and procedures were as described for Experiments 1 and 2 with the following exceptions. In the color naming map shown at the top in Fig. 4, the location marked by the lowest, leftmost square is designated as the (1, 1) test location. Four locations yielding 100/0 ratings — locations (12, 13), (13, 6), (10, 8), and (2, 14) — were designated as L-cone-candidate locations, and three locations producing 0/100 ratings — locations (12, 1), (4, 2), and (9, 6) — were designated M-cone-candidate locations. At each of these locations, probability-of-seeing functions were measured for two wavelengths, 520 and 620 nm after a 40% rod bleach and upon the 460 nm, rod- and S-cone-suppressing background. Threshold was defined as the level producing 80% seen.

4.2. Results

Fig. 5 shows the relative spectral sensitivities to 520 nm as compared to 620 nm at the four L cone candidate locations and the three M cone candidate locations. The mean relative sensitivities, the rod spectral sensitivity, and the Smith and Pokorny (1975) L and M cone spectral sensitivities are also plotted in Fig. 5. The locations — (12, 1), (4, 2), and (9, 6) — which observer CC rated 0/100, entirely green, yielded a mean relative spectral sensitivity in good agreement with the M cone spectral sensitivity. The locations — (12, 13), (13, 6), (10, 8), and (2, 14) — rated 100/0, entirely red, yielded a mean relative spectral sensitivity in reasonable agreement with the L cone spectral sensitivity but lying slightly outside the 95% confidence limits. It should be noted that worse fits to the 100/0 ratings would be obtained with the M cone or rod spectral sensitivities. Thus, overall these comparisons give a measure of confidence in the color naming maps shown in Fig. 4

— red ratings can be linked to quantum catches in L cones and green ratings to M cones.

5. Model based on the ideal observer: from color naming to cone mosaics

The color naming results presented in Fig. 4 give a rough description of the layout of L and M cones in the peripheral retina centered at 17° temporal eccentricity. For example, there are regions in which red ratings dominate, others in which green ratings dominate and still others in which yellow ratings dominate. The regions of red ratings and green ratings are linked to the positions of L or M cones, respectively, by the spectral sensitivity measurements of Experiment 4. Thus, based on a qualitative assessment, the arrangement of L and M cones is not likely to be regular. Can each observer's color naming map be used to estimate the position of every cone in the photoreceptor array producing the color naming results? To answer this question a model based on an ideal observer (Green & Swets, 1966) was used to produce simulated color naming for all possible layouts of L and M cones. The mosaic giving the closest match to each observer's color naming results was chosen as that showing the placements of L and M cones most likely to have produced each individual's color naming maps shown in Fig. 4.

5.1. Description of the model

In its simplest form red–green opponency for *large fields* can be expressed as,

$$pL(\lambda) - qM(\lambda) \tag{1}$$

where $L(\lambda)$ and $M(\lambda)$ represent the cone spectral sensitivities and p and q are weighting coefficients for the different cone inputs to the opponent site (Jameson & Hurvich, 1955). The weighting coefficients p and q combine factors such as the relative numerosity of L and M cones (N_L/N_M) and the different neural weights (k_L and k_M). Explicitly representing these factors in Eq. (1) above, then

$$N_L k_L L(\lambda) - N_M k_M M(\lambda) \tag{2}$$

where $p = N_L k_L$ and $q = N_M k_M$. This general formulation was shown to describe red–green color appearance in central fovea (Cicerone, 1990) for a sample of nine color normal observers and in peripheral retina (Cicerone & Otake, 1997) for a sample of two observers for test sizes illuminating large numbers of cones.

For *small fields* as in this study, each test flash illuminated only one to three cones when assuming a mean cone center-to-center separation of 3 min of arc. At each test location, the model specifies that the color appearance of the 555 nm test stimulus is determined by the illuminated sample of L and M cones numbering n_L and n_M, respectively, according to:

$$k_L \sum_{i=1}^{n_L} L_i(\lambda) - k_M \sum_{j=1}^{n_M} M_j(\lambda) \tag{3}$$

where $L_i(\lambda)$ and $M_j(\lambda)$ are the quantal absorptions in each of the illuminated L or M cones and k_L and k_M are the neural weights applied respectively to the L and M cone inputs at the red–green opponent site. We note that the sample of cones illuminated by each test flash could range from all L cones to all M cones and thus n_L/n_M at each flash location does *not* in general equal the population ratio N_L/N_M.

For each possible combination of illuminated cones at each test location and for a range of different values of the relative neural weights, the model calculated a discrimination index (d')

$$d' = \frac{k_L \sum_{i=1}^{n_L} L_i(\lambda) - k_M \sum_{j=1}^{n_M} M_j(\lambda)}{\sqrt{k_L \sum_{i=1}^{n_L} L_i(\lambda) + k_M \sum_{j=1}^{n_M} M_j(\lambda)}} \tag{4}$$

The value of d' is maximal when the test falls exactly upon an L cone and minimal when it falls exactly upon an M cone. Each calculated d' value was then linked to the color rating scale in the following way (Macmillan & Creelman, 1991). The human observer used 11 categories, ranging from 100% red (category 1) to 50% red, 50% green (category 6) to 100% green (category 11) to classify stimuli varying along the redness–greenness dimension. Analogously, the full range of possible d' values was partitioned into 11 equally-sized subdivisions, corresponding to the 11 categories of percent ratings of color appearance used by the human observers. In addition, the model observer responded 'not seen' if insufficient numbers of quanta, assumed to be less than six (Marriott, 1963; Cicerone & Nerger, 1989), were absorbed in all of the illuminated cones (due to the test falling too far distant from an L or M cone, for example). Accordingly, simulated color naming data were generated and compared, location by location, to the color naming data generated by the human observers for every possible placement of cones.

The model observer assumed the L and M cone spectral sensitivities of Smith and Pokorny (1975) and Geisler's (1984) analytic form for the optical scatter profile based on measurements of Campbell and Gubisch (1966) for a 2 mm pupil. The choice of this optical scatter profile for the present experiments, conducted at 17° eccentricity, is supported by considering the results of Campbell and Gubisch (1966) and a recent study by Navarro et al. (1993). As discussed in Section 1.2, Navarro et al. (1993) find that the aerial point spread is virtually unchanged up to 10° eccentricity with a modest decline in quality at an eccentricity of 20° and significant loss of optical quality only for

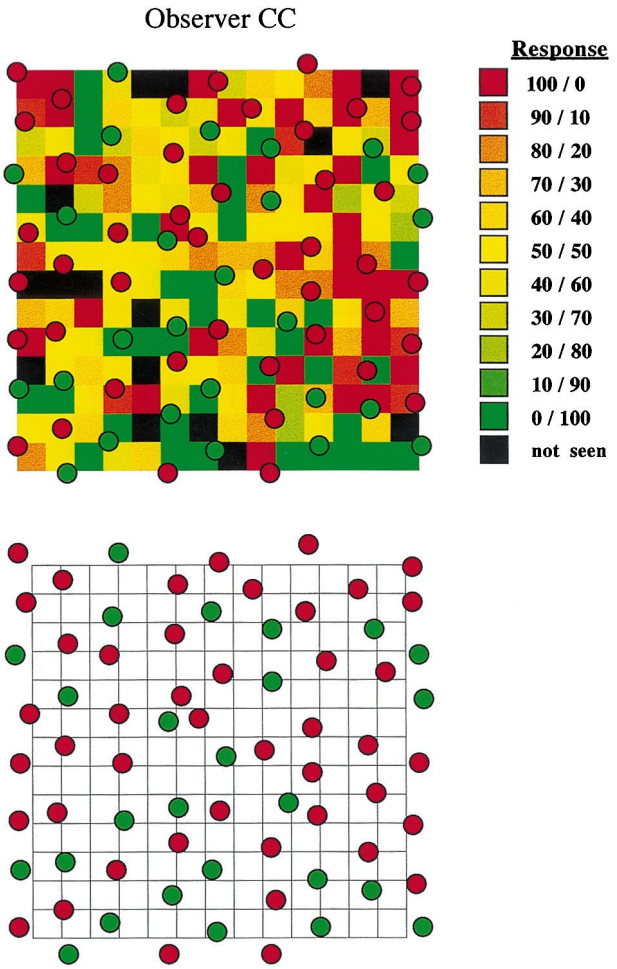

Fig. 6. The cone mosaic shown at the bottom is derived from the model (described in the text) to best match the color naming results of observer CC. The patterns of placement of the 45 L cones (labeled red) and 26 M cones (labeled green) cannot be distinguished from a Poisson random process (95% confidence level). Shown at the top is a comparison of the derived mosaic as compared to the color naming results of observer CC.

eccentricities greater than 30°. Campbell and Gubisch (1966, Fig. 6) report virtually identical linespread functions for 2 and 3 mm diameter pupils and a decline in quality for larger pupil diameters. Our results, collected with a 2.8 mm pupil, should provide some improvement in optical quality as compared to Navarro et al. (1997) whose results were collected with a 4 mm pupil. Hence, Geisler's analytic form for the optical scatter profile of Campbell and Gubisch was chosen.

5.2. Procedure

To keep the computations tractable, it was assumed that the model observer's fixational accuracy was perfect. For our purposes, this assumption is tenable for the following reasons. First, human fixational accuracy, limited by the combined effects of eye tremor and drift, is reported to have a standard deviation near 1 min of arc (e.g. Riggs, Armington & Ratliff, 1954; Fahle, 1991). Second, in the present experiments, the effect of eye tremor was minimized by using fixation aids, briefly flashed tests, and instructions to the observer to self-present test lights when sure of accurate fixation. A separate study (Gowdy & Cicerone, 1998) reports that with these additional factors, the upper limit of the standard deviation of fixational accuracy is small, approximately 82 s of arc for one observer and 54 s of arc for another. Thus, the standard deviation of fixational accuracy is about one-third of the cone-to-cone separation in the region surveyed in this study.

There were at least three possible ways in which the ratio of the L and M cone neural weights at the red-green opponent site could enter into the model. One choice is to set the ratio equal to unity. A second choice is to set the weight equal to that determined by large field unique yellow measurements (Cicerone, 1990). Instead, we chose a third alternative which was to allow the ratio of L and M cone neural weights to vary as a free parameter, thus avoiding the assumption that the neural weights are the same for all observers. In fact, the analysis is relatively insensitive to the ratio of the neural weights, with nearly identical solution mosaics and reasonable fits obtained over a range of values of the ratio (including values close to unity) for one observer. This is a clear indication that the *spatial arrangement* of the L and M cones in the cone array is the primary factor in this model and that the neural weighting is secondary. Although this point is discussed more fully in the section below, we note that when single cones or cones of one class are illuminated by the small test flashes used in these experiments, any differences in neural weights become negligible for the analysis based on our model.

In this peripheral region of the retina, the cone photoreceptors are laid out roughly in a hexagonal array with local departures from perfect hexagonality whose statistical properties have been anatomically estimated (Curcio et al., 1990, 1991). To ease the computational burden, the analysis was broken down into two phases. In the first phase, cone positions were fixed within a perfect hexagonal array with cone center-to-center spacing of 3 min of arc; only their identities as L or M cones were varied. Given the luminance profile of the stimuli, at each test flash location only one to three cones participated in the color rating. (See Section 1.2 above for details.) At each test flash location the model observer calculated d' (Eq. (4)) for every possible set (ranging from 2^1 to 2^3) of L and M assignments to the effectively illuminated cones within the hexagonal array. The calculated value of d' was then mapped into the 11-point color rating scale. That set of L and M cone assignments yielding the best match to the human observer's color rating at that location was selected.

This procedure was then repeated at every test flash location.

Even with the large cone-to-cone separation in this retinal region an individual cone could participate in up to nine color ratings. Therefore, those locations that participated in more than one color rating could potentially have conflicting L or M assignments. For example, the rating for a particular test flash may indicate an L cone assignment whereas for a neighboring test flash an assignment as M cone to that same cone position might be preferred because of the color rating for the second flash. Such discrepant assignments should be few if the color rating map accurately reflects the underlying array of cones. In particular, if fixational accuracy had been poor overall then a large number of discrepant assignments might be expected after this first step of the analysis. In fact, only about 15% of the cone locations showed conflicting assignments, indicating that there is a high degree of spatial consistency in the human observer's color naming for neighboring test locations involving overlapping sets of cones. This location-by-location consistency greatly reduced the calculation burden. Finally, the model was fit to the data by choosing the cone mosaic yielding the smallest value of χ^2 for the comparison between the human observer's set of color ratings and those of the ideal observer based model.

The results of the phase one analysis, using a fixed hexagonal array of cones, yielded a good match between the model observer's and the human observers' color ratings. However, as noted above, the cone mosaic at this retinal eccentricity departs from a perfect hexagonal array in a manner whose statistical properties have been anatomically estimated (Curcio et al., 1990, 1991). To take into account these departures from hexagonal regularity, in the second phase of the analysis cone separations were allowed to vary within the limits set by these anatomical measurements while the L and M assignments from phase one, described above, were kept fixed. Considering all possible directions for repositioning a cone was computationally intractable. We used an iterative search that was restricted to just the six directions of the three cardinal axes of the hexagonal array relative to the cone's starting position at each step of this second phase of the analysis. Furthermore, the iterative search was designed in such a way that directions that worsened the fit were omitted from the analysis at the outset, significantly reducing the number of calculations. Consider a single cone in the hexagonal array. On the first step, we tested the effect of moving that cone 0.5 standard deviation, or 0.3 min of arc (Curcio et al., 1990, 1991), along each of the six cardinal directions relative to the initial position of the cone. If any one of those repositionings improved the χ^2 fit as compared to its previous location, then the cone was moved to that new location. On the second step, this procedure was repeated, except that it was not necessary to test three of the possible repositionings tested in step one. Again, if a repositioning improved the χ^2 fit then the cone was moved to that new location. Step two was repeated twice more. Following this regimen, a cone could move a maximum of 2 standard deviations (1.2 min of arc) from its original array location. Note that the line between the cone's initial and ultimate resting positions need not be coincident with any of the cone's original cardinal axes of step one, because the cardinal axes for a cone were updated as it was relocated. Following this set of procedures *en masse* for all possible combinations of all the cones in the mosaic would be prohibitive; this was not necessary because well-separated sets of cones never participate in the same color rating of these small, brief flashes, each illuminating at most three cones. Therefore, the whole mosaic could be subdivided and separately analyzed. Only cones on the borders of subdivisions participated in the same color ratings and required testing for conflicting repositionings. In fact, only a handful of cone locations showed conflicting repositionings, indicating once again that there is a high degree of spatial consistency in the human observer's color naming. To resolve any conflicts at the borders of subdivisions, the repositionings giving the smallest value of χ^2 were chosen.

5.3. Results

The cone mosaics yielding the best match (χ^2) between the model and the experimental results are shown against the color ratings in Figs. 6 and 7. It is noted that cone assignments can be made at locations where the test is not seen by using information at neighboring locations. Observer CC's mosaic (obtained with $k_M/k_L = 2.0$) consists of 45 L and 26 M cones yielding a ratio near 1.7. Observer KL's mosaic (obtained with $k_M/k_L = 1.9$) is composed of 47 L and 25 M cones yielding a ratio near 1.9. On each simulated trial, all cones illuminated by the tiny test can be designated in whatever combination, from all L to all M, to obtain the best fit to the human observer's responses. Thus, the L and M cone relative numerosity estimated in this study is a result of the modeling applied to the color naming data, not an assumption of the model. These estimates of L and M cone relative numerosity are in good agreement with previous estimates, 2.1 in fovea for Observer CC (Cicerone & Nerger, 1989) and 1.9 in fovea and 2.0 at 17° nasal eccentricity for Observer KL (Cicerone & Otake, 1997) based on different methods. In agreement with Hagstrom et al. (1998), the present results do not indicate a change in the L to M cone relative numerosity between fovea and 17° eccentricity.

The spectral sensitivities measured at L and M cone candidate locations in Experiment 3 can be compared

to the positions of specific cones in the derived mosaics based on the model. In Experiment 2 for Observer CC, test locations (12, 1), (4, 2), and (9, 6) produced ratings of 0/100 and test locations (12, 13), (13, 6), (10, 8), and (2, 14) ratings of 100/0. Spectral sensitivity measurements at those locations (Experiment 3) yielded consistent results: Locations of 0/100 color ratings yielded a best match to M cone spectral sensitivity; and 100/0 ratings were best matched to L cone spectral sensitivity. As another check for consistency in the present results, cones located nearest test locations judged 100/0 or 0/100 should be L or M cones, respectively. This comparison can be made by inspecting the derived mosaic superimposed upon the color naming results at the top of Fig. 6. The convention established above of specifying the center of the square at the lower, left corner as test location (1, 1) is used. For the M cone candidate locations from the results of Experiments 2 and 3, test location (12, 1) lies among M cones; location (4, 2) lies among two M cones and one L cone; and an M cone is

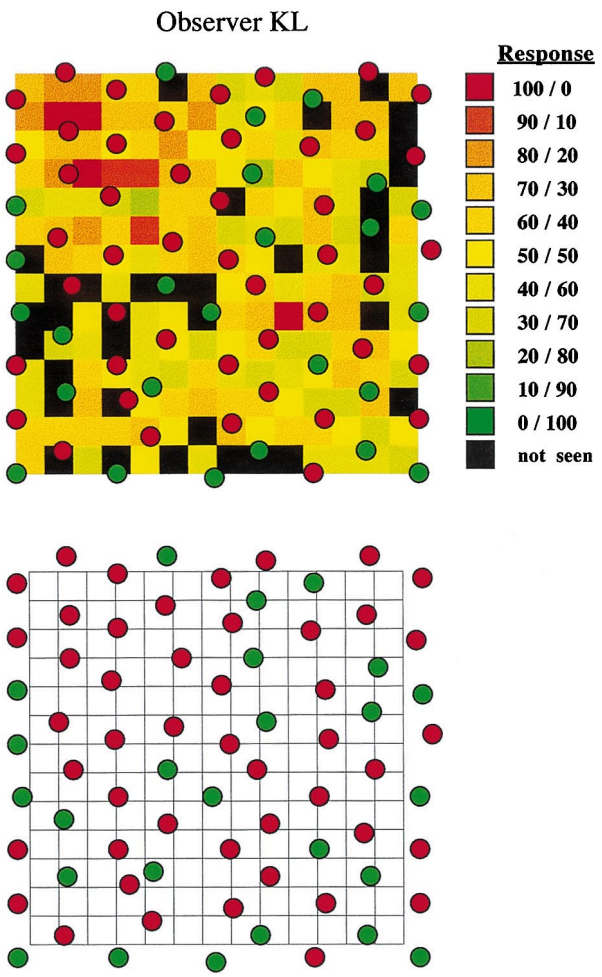

Fig. 7. Shown are results for observer KL. All symbols and explanations are as for Fig. 6. Observer KL's mosaic consisted of 47 L and 25 M cones whose pattern of placement cannot be distinguished from a Poisson random process (95% confidence level).

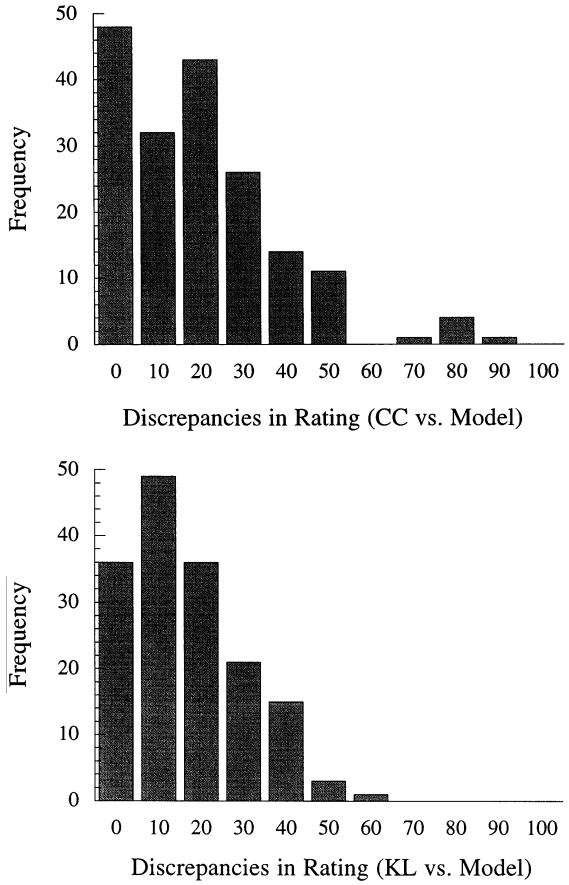

Fig. 8. The discrepancies between each human observer's and the model observer's color ratings are summarized. Frequency histograms of the number of locations producing discrepancies ranging from 0 to 100% in units of the rating scale for observers CC (top) and KL (bottom) are shown.

the nearest cone for location (9, 6) in the derived mosaic; location (9, 6) is one surrounded by L cones, except for a single M cone located nearest to it. For the L cone candidate locations from the results of Experiments 2 and 3, an L cone lies near test location (12, 13); location (13, 6) is surrounded by L cones; an L cone lies nearly at location (10, 8); and an L cone is the closest cone to location (2, 14). Thus, the model tends to be validated by the agreement between locations of L or M cones in the derived mosaic and color naming observation and spectral sensitivity measurements.

The discrepancies between each human observer's and the model observer's color ratings at 196 test locations are summarized in Fig. 8. Shown are frequency histograms for observers CC (top) and KL (bottom) of the number of test locations producing discrepancies ranging from zero to 100% in units of the color rating scale. Observer CC and the model observer, basing its responses on the derived mosaic (Fig. 4, top), disagreed by no more than 10% on roughly half of the test locations, and there were few discrepancies over 50%. It is noted that there are a handful of

locations with large discrepancies ranging from 70 to 90%. For example, at location (13, 4) the human observer CC made a strongly green response, but the model observer responded strongly red because of the L cone located there. These locations of large discrepancies comprise a small fraction, six out of 196, of the total observations for observer CC. Observer KL's comparison to the model observer's responses based on KL's mosaic (Fig. 4, bottom) shows even less discrepancy with none of magnitude 60% or greater.

5.4. Results of test–retest comparisons

As another check of the combined color naming experiments and modeling, this methodology was applied separately to two sets of observations, collected in different sessions at the same retinal region for the same human observer. If the methodology is robust, then the cone arrays obtained by means of the analysis should be reasonably similar. Such a comparison is shown in Fig. 9 for observer CC. Two sets of color naming results were collected in separate sessions (top) and their associated cone mosaics (bottom) were derived with the aid of the model. Observations labeled test (left) and retest (right) were made in the same retinal region centered at 17° temporal eccentricity. The cone mosaic based on the retest differs from that based on the original observations by nine cones out of 72. These nine cones are highlighted by dark rings. The identities of the rest of the cones (88%) are the same in the two mosaics and the departures from strict hexagonal arrangements of the cones in the two mosaics are

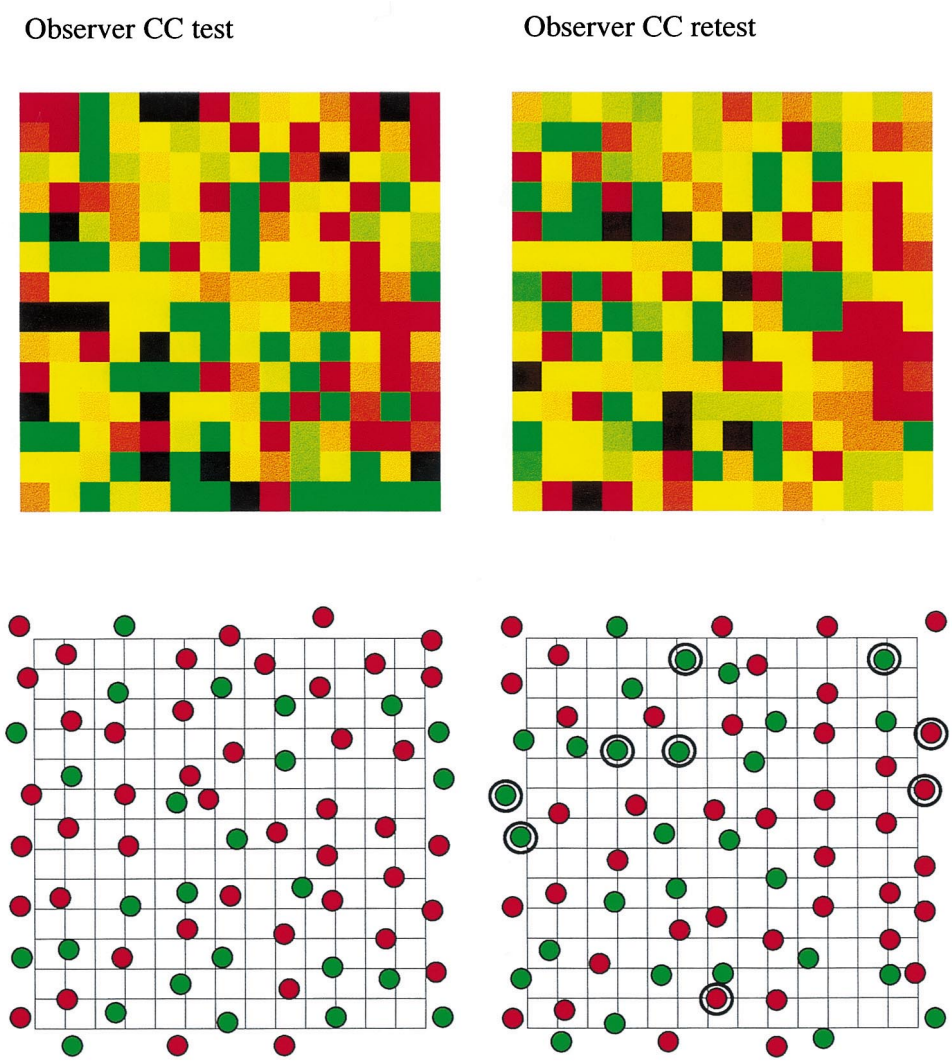

Fig. 9. Shown are two sets of color naming results for observer CC collected in separate sessions (top) and their associated cone mosaics (bottom) derived with the aid of the model described in the text. Observations labeled test (left) and retest (right) were made in the same retinal region. The cone mosaic based on the retest differs from that based on the original observations by nine cones out of 72. These nine cones are highlighted by dark rings. The identities of the rest of the cones (88%) are the same in the two mosaics and the departures from a strict hexagonal arrangement of the cones in the two mosaics are also similar.

also similar. It seems reasonable to conclude that the mosaics based on the test and retest are in good agreement.

5.5. Distribution scheme of the cone arrays in peripheral retina

Ripley's (1981) *L* statistic was used to determine whether the L and M cone arrays in each observer's mosaic (Figs. 6 and 7) differed significantly from the expectations of a random distribution. This statistic was used because, as was confirmed by test runs, it can distinguish among regular, clumped, and random arrays under the assumptions of homogeneity and isotropy. These assumptions are likely to hold at 17° temporal eccentricity because cone density is roughly constant in this region of the retina (Curcio et al., 1990). The *L* statistic (based on a frequency count of the distances of each cone to its nearest like-type neighbor) was calculated separately for the L and M cones for each observer's mosaic. The *L* statistics derived from the observer's mosaic were then compared to the expected results based on 500 mosaics generated with random placement of the different cone classes represented in numbers matched to those in the observer's mosaic. This analysis indicated that the patterns of placement of separate L and M cones in each observer's mosaics are not significantly different from the expectations of a Poisson random process (95% confidence level).

6. Discussion

6.1. Consequences of various distribution schemes for the different cone classes

The distribution of the L and M cones is not significantly different from random for the peripheral photoreceptor matrix in two color normal eyes of this study. This finding coincides with that of a companion study on the spatial arrangement of L and M cones in the central fovea of two human eyes (Gowdy & Cicerone, 1998) and with the findings at 1° nasal eccentricity in one of two eyes in the recent study by Roorda and Williams (1999). We suggest that a random distribution of cone types might represent a spatial and spectral sampling scheme that is a compromise between regular and clumped arrays of cones. A high degree of clumping is likely to produce poor chromatic sampling across the visual scene but good cone-specific spatial resolution within clumps of like-type cones. By comparison, a regular array is characterized by better chromatic sampling across the visual scene but poorer cone-specific spatial resolution, especially in the peripheral retina where the cones are rather sparsely distributed. Random mosaics should tend to be characterized by different patterns in different regions; by chance, in some regions there is likely to be some degree of clumping and in others some degree of dispersion among like-type cones.

If the L and M cones are interleaved in a regular array, a straight-forward expectation is that acuity based on the L or M cone submosaics should be worse than that based on the full mosaic. A number of studies of foveal acuity based on grating stimuli (e.g. Green, 1968; Cavonius & Estevez, 1975) or laser interference fringes (Williams, 1990) show that the acuity based on either cone class alone is no poorer than that based on the full cone mosaic. This finding can be explained either if the array is regular and some sort of postreceptoral processing exploits any correlations in the signals from the L and M cones (Williams, Sekiguchi, Haake, Brainard & Packer, 1991) or if clumps of like-type cones provide acuity based on the L or M cone submosaics equal to that based on the full mosaic.

Clumping is likely to be a poor scheme for producing color opponent receptive fields. There is good agreement that the centers of color opponent receptive fields in the fovea are fed by a single cone type (e.g. Wiesel & Hubel, 1966; Boycott & Dowling, 1969; Shapley & Perry, 1986; Boycott & Wässle, 1991). Whether their surrounds receive inputs from a single cone type (e.g. Wiesel & Hubel, 1966; Shapley, Reid & Kaplan, 1991; Reid & Shapley, 1992; Masland, 1996) or mixed cone types (e.g. Paulus & Kröger-Paulus, 1983; Young & Marrocco, 1989; Lennie, Haake & Williams, 1991; DeValois & DeValois, 1993), clumping of cones would interfere with the formation of color-opponent receptive field surrounds in clumped regions because inputs to the surrounds from cone types different from those of the center must be drawn from distant retinal regions. On the other hand, either random or regular placements of cone types would more easily allow the formation of color opponency (e.g. Paulus & Kröger-Paulus, 1983; Young & Marrocco, 1989; DeValois & DeValois, 1993). Hence, a random scheme for the interleaving of the L and M cones may best provide for the dual requirements of color opponency and spatial resolution because random distributions tend to be characterized by regions of moderate clumping and other regions of near regularity.

6.2. L and M cone numerosity and color appearance in the peripheral retina

The relative numerosity of L and M cones estimated at 17° temporal eccentricity in this study (1.7 for CC and 1.9 KL) is within the range of foveal (Cicerone & Nerger, 1989) and parafoveal values (Nerger & Cicerone, 1992) obtained in this laboratory. Thus, in addition to a randomly distributed array of L and M

cones, a secondary conclusion of this study is that the relative numbers of L and M cones is not different at 17° temporal eccentricity as compared to the fovea centralis and parafovea.

Some earlier psychophysical results appeared to provide indirect evidence that the relative numbers of L and M cones was not stable with eccentricity. Measurements of color appearance (e.g. Boynton, Schafer & Neun, 1964), wavelength discrimination (e.g. Weale, 1951), and spectral sensitivity (e.g. Uchikawa, Kaiser & Uchikawa, 1982) based on small, dim test lights showed decreased M cone sensitivity in the peripheral retina and could be interpreted as support for the conclusion that there is a decrease in the relative numbers of M cones in the periphery. An alternative explanation of the results is that small, dim tests produce fewer quantal absorptions in M cones as compared to L cones because of three factors: (1) the relatively large cone-cone separations in peripheral retina; (2) a random distributions of L and M cones; and (3) a relative numerosity favoring L as compared to M cones. This interpretation is consistent with recent psychophysical reports showing that a full range of well-saturated hues can be observed in the extreme periphery if the intensity and size of the test stimuli are appropriately scaled with eccentricity (e.g. Abramov et al., 1991; Hibino, 1992; Nerger, Volbrecht & Ayde, 1995). In addition, Stabell and Stabell (1984) demonstrated that the photopic luminous efficiency function remains constant with eccentricity, if test fields are scaled to account for the cortical magnification factor and macular pigmentation. There is ample evidence that the photopic luminous efficiency function is a combination of the L and M cone quantum catches scaled by their relative numbers (De Vries, 1946; Smith & Pokorny, 1972; Eisner & MacLeod, 1988; Cicerone & Nerger, 1989). Thus, the stability of the photopic luminosity function with eccentricity is consistent with a stable L to M cone ratio with eccentricity. It should be noted that results from studies on L and M pigment gene expression indicate that this stability may not be maintained in the far periphery (Hagstrom et al., 1998).

6.3. The neural weighting of the cone contributions into the red–green color opponent site

The small tests used in the experiment illuminated from one to three cones on any trial. When single cones or cones of one class determine the color rating, any differences in neural weights become immaterial to the analysis based on our model. It is only on those trials in which a mix of L and M cones are illuminated that the relative neural weights at the opponent site is of consequence. There were two possible choices for the treatment of the values of the neural weights k_L and k_M in the model: The ratio of the neural weights could have been set to a constant value equal to that obtained from previous measurements of unique yellow (Cicerone, 1990) or allowed to vary so as to obtain the best fit for each individual's data and to provide an independent estimate of the ratio of neural weights. We chose the latter alternative because this course involved one less assumption about the nature of the red–green opponent site and avoided the presupposition that the neural weights should be the same for all observers. Indeed, heterozygous carriers for X-linked color vision deficiencies with extreme L to M cone ratios show no differences in judged red–green color appearance as compared to normals (Mollon & Jordan, 1995; Miyahara, Pokorny, Smith, Baron & Baron, 1998). These results indicate that, in order to maintain red–green color appearance near the norm, the cone ratios and the values of the neural weightings k_L and k_M into the red–green opponent site may show sizable differences in some individuals. Hence, in our model the neural weights were allowed to vary as free parameters to obtain the best fit between each observer's color naming results and the simulated performance of the model observer, as determined by the smallest value of χ^2.

The relative value of the neural weights, k_M/k_L, producing the best fits were 2.0 for CC and 1.9 for KL. In order to explore the effects of changes in the neural weights on the selection of the mosaic that best fits each human observer's performance, the mosaics resulting from different fixed values of k_M/k_L were compared. We note here once again that for each value of the relative neural weights tested, all possible L and M cone mosaics, ranging from all L to all M, were evaluated. For observer CC similar mosaics were obtained with values of k_M/k_L ranging between 1.5 and 3.0, and for observer KL similar mosaics were obtained with values of k_M/k_L ranging between 1.6 and 2.2. For example, there was little change in the relative numbers of L to M cones (mean value 2.1, standard deviation of 0.12) as k_M/k_L was varied between 1.5 and 3.0 in steps of 0.1 for observer CC's results. Outside this range, the fits were worse and the derived mosaics departed from the best-fitting, solution mosaic. This is a good indication that the dominating factor in the analysis of this study is whether the small test light illuminated only L, only M, or a combination of L and M cones on successive trials and that the neural weighting is secondary. One reason why the values of the neural weights do not have a greater effect on the mosaics derived in this analysis for observer CC is as follows: The experimental conditions were designed so that a small number (one to three) of cones contribute to color naming on each trial. The value of the relative neural weight influences the analysis on those trials involving both L and M cones. Because many trials involve only L or only M cone(s), the overall analysis is relatively insensitive to the value of the relative neural

Table 1
Nearest neighbor distance statistics

	This study 17° (temporal)		Curcio et al. (1991) 10° (see text)
	Observer CC	Observer KL	Retina B4
L/M–L/M			
Mean	2.35	2.55	1.94
S.D.	0.38	0.36	0.20
L–L			
Mean	2.63	2.74	
S.D.	0.57	0.33	
M–M			
Mean	3.00	3.32	
S.D.	0.46	0.90	

weight for observer CC. Observer KL's results show a narrower range of acceptable values of the ratios of the neural weights, in line with his color naming results with few 100/0 and no 0/100 ratings, indicating that on most trials both L and M cones were activated.

According to the foregoing discussion, the present study is not the ideal one to obtain estimates of the L and M cone neural weights as they contribute to the red–green opponent site. The results based on the model of this study are not greatly affected by the relative neural weights; good fits and similar solution mosaics are obtained within a range of values lying between 1.5 and 3.0, and a reasonable fit is obtained even with equal neural weights for L and M cones. Nonetheless, we can compare the values obtained in this study to other estimates in the literature. Cicerone (1990) linked measurements of the *relative numerosity* of L and M cones (ranging between 1.5 and 2.6) to measurements of unique yellow (ranging between 571 and 590 nm) by a single value of the *relative neural weight*, $k_M/k_L = 2.8$, for all individuals in a sample of nine observers. The color naming task used a suprathreshold test, 0.25° in diameter, illuminating at least 700 foveal cones. Given the differences in the test sizes, this value of k_M/k_L is in reasonable agreement with the results of the present study.

Sankeralli and Mullen (1996) used the results of a detection task and $pL(\lambda) - qM(\lambda)$ as the formulation for the red–green opponent mechanism (Eq. (1), above) to estimate that p/q is near unity. The color appearance task of the present study and a detection task may not tap into the color-opponent pathway at the same point. Nonetheless, given that the test lights in the present experiments were set near a conventional detection threshold (80% seen), it seemed reasonable to expect similar values of p/q for the observers in this study. On the basis of the development above (Eqs. (1) and (2)), the p/q values for this study can be calculated from the L to M cone ratio in the derived mosaics and the cone neural weights providing the best fits. Observer CC's mosaic with 45 L and 21 M cones based on $k_M/k_L = 2.0$ yields a value of $p/q = 1.07$. Observer KL's mosaic with 43 L and 23 M cones based on $k_M/k_L = 1.9$ yields a value of $p/q = 0.98$. These values of p/q are in good agreement with those of Sankeralli and Mullen (1996).

6.4. Spatial statistics of the cone mosaics

The most eccentric region for which the anatomical studies of Curcio et al. (1991) provide spatial statistics is located at 10° eccentricity within the boundaries of the temporal and superior-temporal meridians (personal communication). For L and M cones considered as a single class (L cones were not distinguished from M cones in the study of Curcio et al.), the mean separation between cones, either L or M, was 1.94 ± 0.20 min of arc for Retina B4 (Table 1). If this value is scaled according to cone density at 17° eccentricity, then a value of 2.61 ± 0.27 is obtained. This compares reasonably well to the values of 2.35 ± 0.38 for Observer CC's mosaic and 2.55 ± 0.36 for Observer KL's mosaic (Table 1). The larger variability in the derived mosaics of the present study as compared to the anatomical results is likely due to the smaller sample size of cones in the present study.

For the cone mosaics of both observers CC and KL, the model produced sizable gaps in the L and M cone array in order to best account for the color naming observations. Our methodology, aimed at estimating the L and M cone subarrays, sought to exclude any other photoreceptor type from participation in the experimental task. Thus, we can only speculate that these gaps may correspond to the locations of S cones in the overall cone array. In support of this speculation, it is noted that the number of gaps (four for CC and three for KL) and their spacing correspond roughly to the expectations of the spatial statistics for S cones in this region of the retina as determined by anatomical means (Ahnelt et al., 1987; Curcio et al., 1991).

6.5. Cross-species comparisons

A numerical superiority of L cones as compared to M cones agrees with other measurements in humans (De Vries, 1946, 1948; Vos & Walraven, 1971; Cicerone & Nerger, 1989; Vimal et al., 1989; Cicerone, 1990; Nerger & Cicerone, 1992; Hagstrom et al., 1997; Gowdy & Cicerone, 1998; Roorda & Williams, 1999) but is inconsistent with the reverse finding in baboon (Marc & Sperling, 1977) and the finding of roughly equal numbers in talopoin (Mollon & Bowmaker, 1992) and macaque (Packer et al., 1996). The conclusion that L and M cones are randomly interleaved in the cone mosaic is in agreement with the results of Marc and

Sperling (1977) and Mollon and Bowmaker (1992) for the nonhuman primate retina but is inconsistent with the results of Packer et al. (1996) who find clumping of like-type cones. In a separate study Gowdy and Cicerone (1998) report results of experiments that are consistent with a numerical superiority of L cones as compared to M cones, randomly arrayed in the human foveal cone mosaic.

Acknowledgements

This work was supported by grant EY11132 (PHS-NIH National Eye Institute) to CMC.

References

Abramov, I., Gordon, J., & Chan, H. (1991). Color appearance in the peripheral retina: Effects of stimulus size. *Journal of the Optical Society of America A*, *8*, 404–414.

Aguilar, M., & Stiles, W. S. (1954). Saturation of the rod mechanism of the retina at high levels of stimulation. *Optica Acta*, *1*, 59.

Ahnelt, P. K., Kolb, H., & Pflug, R. (1987). Identification of a subtype of cone photoreceptor, likely to be blue sensitive, in the human retina. *The Journal of Comparative Neurology*, *255*, 18–34.

Alpern, M. (1971). Rhodopsin kinetics in the human eye. *Journal of Physiology*, *217*, 447–471.

Arden, G. B., & Weale, R. A. (1954). Nervous mechanisms and dark adaptation. *Journal of Physiology* (*London*), *125*, 417.

Boycott, B. B., & Dowling, J. E. (1969). Organization of the primate retina: light microscopy. *Philosophical Transactions of the Royal Society B*, *255*, 109–184.

Boycott, B. B., & Wässle, H. (1991). Morphological classification of bipolar cells of the primate retina. *European Journal of Neuroscience*, *3*, 1069–1088.

Boynton, R. M., & Gordon, J. (1965). Bezold-Brücke hue shift measured by color-naming technique. *Journal of the Optical Society of America*, *55*, 78–86.

Boynton, R. M., Schafer, W., & Neun, M. E. (1964). Hue-wavelength relation measured by color-naming method for three retinal locations. *Science*, *146*, 666–668.

Campbell, F. W., & Gubisch, R. W. (1966). Optical quality of the human eye. *Journal of Physiology*, *186*, 558–578.

Castaño, J. A., & Sperling, H. (1982). Sensitivity of the blue-sensitive cones across the central retina. *Vision Research*, *22*, 661–673.

Cavonius, C. R., & Estevez, O. (1975). Contrast sensitivity of individual colour mechanisms of human vision. *Journal of Physiology*, *248*, 649–662.

Cicerone, C. M., Krantz, D. H., & Larimer, J. (1975). Opponent-process additivity. III. Effect of moderate chromatic adaptation. *Vision Research*, *15*, 1125–1135.

Cicerone, C. M. (1990). Color appearance and the cone mosaic in trichromacy and dichromacy. In Y. Ohta, *Colour vision deficiencies* (pp. 1–12). The Netherlands: Kugler & Ghedini.

Cicerone, C. M., & Nerger, J. L. (1989). The relative numbers of long-wavelength-sensitive to middle-wavelength-sensitive cones in the human fovea centralis. *Vision Research*, *29*, 115–128.

Cicerone, C. M., & Otake, S. (1997). Color-opponent sites: individual variability and changes with retinal eccentricity. *Investigative Ophthalmology and Visual Science*, *38* (Suppl.), 2130 (Abstract).

Curcio, C. A., Allen, K. A., Sloan, K. R., Lerea, C. L., Hurley, J. B., Klock, I. B., & Milam, A. H. (1991). Distribution and morphology of human cone photoreceptors stained with anti-blue opsin. *The Journal of Comparative Neurology*, *312*, 610–624.

Curcio, C. A., Sloan, K. R., Kalina, R. E., & Hendrickson, A. E. (1990). Human photoreceptor topography. *The Journal of Comparative Neurology*, *292*, 497–523.

DeValois, R. L., & DeValois, K. K. (1993). A multi-stage color model. *Vision Research*, *33*, 1053–1065.

DeValois, R. L. (1965). Analysis and coding of color vision in the primate visual system. *Cold Spring Harbor Symposium on Quantitative Biology*, *30*, 567–579.

De Vries, H. L. (1946). Luminosity curve of trichromats. *Nature*, *157*, 736–737.

De Vries, H. L. (1948). The heredity of the relative numbers of red and green receptors in the human eye. *Genetica*, *24*, 199–212.

Eisner, A. E., & MacLeod, D. I. A. (1988). Flicker photometric study of chromatic adaptation: selective suppression of cone inputs by colored backgrounds. *Journal of the Optical Society of America*, *71*, 705–718.

Fahle, M. (1991). Psychophysical measurements of eye drifts and tremor by dichoptic or monocular vernier acuity. *Vision Research*, *31*, 209–222.

Fick, A. E. (1888). Studien über Licht- und Farbenempfindung. *Pflüger's Archiv für die gesamte Physiologie des Menschen und der Tiere*, *43*, 441–501.

Geisler, W. S. (1984). Physical limits of acuity and hyperacuity. *Journal of the Optical Society of America A*, *1*, 775–782.

Gowdy, P. D., & Cicerone, C. M. (1998). The spatial arrangement of the L and M cones in the central fovea of the living human eye. *Vision Research*, *38*, 2575–2589.

Green, D. G. (1968). The contrast sensitivity of the colour mechanisms of the human eye. *Journal of Physiology*, *196*, 415–429.

Green, D. M., & Swets, J. A. (1966). *Signal detection theory and psychophysics*. New York: Wiley.

Hagstrom, S. A., Neitz, J., & Neitz, M. (1998). Variations in cone populations for red–green color vision examined by analysis of mRNA. *Neuroreport*, *9*, 1963–1967.

Hartridge, H. (1947). The visual perception of fine detail. *Philosophical Transactions Series B*, *232*, 519.

Hecht, S., Haig, C., & Chase, P. M. (1937). The influence of light-adaptation on subsequent dark-adaptation of the eye. *Journal of General Physiology*, *20*, 831.

Hibino, H. (1992). Red–green and yellow–blue opponent-color responses as a function of retinal eccentricity. *Vision Research*, *32*, 1955–1964.

Holmgren, F. (1884). Über den Farbensinn. *Compte rendu du congrès périodique international des sciences médicales Copenhagen*, *1*, 80–98.

Holmgren, F. (1889). Studien über die elementaren Farbenempfindungen. *Skandinavisches Archiv für Physiologie*, *1*, 152–182.

Jameson, D., & Hurvich, L. M. (1955). Some quantitative aspects of an opponent-colors theory — I: chromatic responses and spectral saturation. *Journal of the Optical Society of America*, *45*, 546–552.

Krauskopf, J. (1964). Color appearance of small stimuli and the spatial distribution of color receptors. *Journal of the Optical Society of America*, *54*, 1171.

Larimer, J., Krantz, D. H., & Cicerone, C. M. (1974). Opponent-process additivity I. Red/green equilibria. *Vision Research*, *14*, 1127–1140.

Lennie, P., Haake, P. W., & Williams, D. R. (1991). The design of chromatically opponent receptive fields. In M. S. Landy, & J. A. Movshon, *Computational models of visual processing* (pp. 71–82). Cambridge, MA: MIT Press.

Macmillan, N. A., & Creelman, C. D. (1991). *Detection theory: A user's guide*. Cambridge: Cambridge University Press.

MacLeod, D. I. A., & Boynton, R. M. (1979). Chromaticity diagram showing cone excitation by stimuli of equal luminance. *Journal of the Optical Society of America*, *69*, 1183–1186.

Marc, R. E., & Sperling, H. G. (1977). Chromatic organization of primate cones. *Science*, *196*, 454–456.

Marks, W. B., Dobelle, W. H., & MacNichol, E. F. (1964). Visual pigments of single primate cones. *Science*, *1434*, 1181–1183.

Marriott, F. H. C. (1963). The foveal absolute visual threshold for short flashes and small fields. *Journal of Physiology* (*London*), *169*, 416–423.

Masland, R. H. (1996). Unscrambling color vision. *Science*, *271*, 616–617.

McKee, S. P., & Levi, D. M. (1987). Dichoptic hyperacuity: the precision of nonius alignment. *Journal of the Optical Society of America A*, *4*, 1104–1108.

Miyahara, E., Pokorny, J., Smith, V. C., Baron, R., & Baron, E. (1998). Color vision in two observers with highly biased LWS/MWS cone ratios. *Vision Research*, *38*, 601–612.

de Monasterio, F. M., Schein, S. J., & McCrane, E. P. (1981). Staining of blue-sensitive cones of the macaque retina by fluorescent dye. *Science*, *213*, 1278–1281.

Mollon, J. D., & Bowmaker, J. K. (1992). The spatial arrangement of cones in the primate fovea. *Nature*, *360*, 677–679.

Mollon, J. D., & Jordan, G. (1995). Is unique yellow related to the relative numerosity of L and M cones? *Investigative Ophthalmology and Visual Science*, *36* (Suppl.), 189 (Abstract).

Nathans, J., Thomas, D., & Hogness, D. S. (1986). Molecular genetics of human color vision: The genes encoding blue, green, and red pigments. *Science*, *232*, 193–202.

Navarro, R., Artal, P., & Williams, D. R. (1993). Modulation transfer of the human eye as a function of retinal eccentricity. *Journal of the Optical Society of America A*, *10*, 201–212.

Nerger, J. L., & Cicerone, C. M. (1992). The ratio of L cones to M cones in the human parafoveal retina. *Vision Research*, *32*, 879–888.

Nerger, J. L., Volbrecht, V. J., & Ayde, C. J. (1995). Unique hue judgments as a function of test size in the fovea and at 20-deg temporal eccentricity. *Journal of the Optical Society of America A*, *12*, 1225–1232.

Østerberg, G. (1935). Topography of the layer of rods and cones in the human retina. *Acta Ophthalmology* (*Suppl*), *6*, 1–103.

Packer, O. S., Williams, D. R., & Bensinger, D. G. (1996). Photopigment transmittance imaging of the primate photoreceptor mosaic. *The Journal of Neuroscience*, *16*, 2251–2260.

Paulus, W., & Kröger-Paulus, A. (1983). A new concept of retinal colour coding. *Vision Research*, *23*, 529–540.

Reid, R. C., & Shapley, R. M. (1992). Spatial structure of cone inputs to receptive fields in primate lateral geniculate nucleus. *Nature*, *356*, 716–718.

Riggs, L. A., Armington, J. C., & Ratliff, F. (1954). Motions of the retinal image during fixation. *Journal of the Optical Society of America*, *44*, 315–321.

Ripley, B. D. (1981). *Spatial statistics*. New York: John Wiley & Sons.

Roorda, A., & Williams, D. R. (1999). The arrangement of the three cone classes in the living human eye. *Nature*, *397*, 520–522.

Sankeralli, M. J., & Mullen, K. T. (1996). Estimation of the L-, M-, and S-cone weights of the postreceptoral detection mechanisms. *Journal of the Optical Society of America A*, *13*, 906–915.

Schnapf, J. L., Kraft, T. W., & Baylor, D. A. (1987). Spectral sensitivity of human cone photoreceptors. *Nature*, *325*, 439–441.

Schnapf, J. L., Nunn, B. J., Meister, M., & Baylor, D. A. (1990). Visual transduction in cones of the monkey Macaca Fascicularis. *Journal of Physiology*, *427*, 681–713.

Shapley, R., & Perry, V. H. (1986). Cat and monkey retinal ganglion cells and their visual functional roles. *Trends in Neuroscience*, *9*, 229–235.

Shapley, R., Reid, R. C., & Kaplan, E. (1991). Receptive field structures of P and M cells in the monkey retina. In A. Valberg, & B. B. Lee, *From pigments to perception: Advances in understanding visual processes* (pp. 95–104). New York: Plenum Press.

Smith, V. C., & Pokorny, J. (1972). Spectral sensitivity of colorblind observers and the cone pigments. *Vision Research*, *12*, 2059–2071.

Smith, V. C., & Pokorny, J. (1975). Spectral sensitivity of the foveal cone photopigments between 400 and 500 nm. *Vision Research*, *15*, 161–171.

Stabell, U., & Stabell, B. (1984). Color-vision mechanisms of the extrafoveal retina. *Vision Research*, *24*, 1969–1975.

Stockman, A. S., MacLeod, D. I. A., & Johnson, N. E. (1993). Spectral sensitivities of the human cones. *Journal of the Optical Society of America A*, *10*, 2491–2521.

Uchikawa, H., Kaiser, P. K., & Uchikawa, K. (1982). Color discrimination perimetry. *Color*, *7*, 264–272.

Vimal, R. L. P., Pokorny, J., Smith, V. C., & Shevell, S. K. (1989). Foveal cone thresholds. *Vision Research*, *29*, 61–78.

Vos, J. J., & Walraven, P. L. (1971). On the derivation of the foveal receptor primaries. *Vision Research*, *11*, 799–818.

Walraven, P. L. (1962). *On the mechanisms of colour vision*. Soesterberg: University of Utrecht.

Weale, R. A. (1951). Hue-discrimination in para-central parts of the human retina measured at different luminance levels. *Journal of Physiology London*, *113*, 115–122.

Wiesel, T. N., & Hubel, D. H. (1966). Spatial and chromatic interactions in the lateral geniculate body of the Rhesus monkey. *Journal of Neurophysiology*, *29*, 1115–1156.

Williams, D. R. (1988). Topography of the foveal cone mosaic in the living human eye. *Vision Research*, *28*, 433–454.

Williams, D. R. (1990). The invisible cone mosaic. In *Advances in photoreception: Proceedings of a symposium on frontiers of visual science* (pp. 135–148). Washington, DC: National Academy Press.

Williams, D. R., MacLeod, D. I. A., & Hayhoe, M. M. (1981). Punctate sensitivity of the blue-sensitive mechanism. *Vision Research*, *21*, 1357–1375.

Williams, D. R., Sekiguchi, N., Haake, W., Brainard, D., & Packer, O. (1991). The cost of trichromacy for spatial vision. In A. Valberg, & B. B. Lee, *From pigments to perception: Advances in understanding visual processes* (pp. 11–22). New York: Plenum Press.

Young, R. A., & Marrocco, R. T. (1989). Predictions about chromatic receptive fields assuming random cone connections. *The Journal of Theoretical Biology*, *141*, 23–40.